Composite Polymer Electrolyte Containing Ionic Liquid and Functionalized Polyhedral Oligomeric Silsesquioxanes for Anhydrous PEM Applications

Surya Subianto,[†] Mayur K. Mistry,[†] Namita Roy Choudhury,*[,†] Naba K. Dutta,[†] and Robert Knott[‡]

Ian Wark Research Institute, University of South Australia, Mawson Lakes, South Australia, and Australian Nuclear Science and Technology Organisation, Menai, New South Wales, Australia

ABSTRACT A new type of supported liquid membrane was made by combining an ionic liquid (IL) with a Nafion membrane reinforced with multifunctional polyhedral oligomeric silsesquioxanes (POSSs) using a layer-by-layer strategy for anhydrous proton-exchange membrane (PEM) application. The POSS was functionalized by direct sulfonation, and the sulfonated POSS (S-POSS) was incorporated into Nafion 117 membranes by the infiltration method. The resultant hybrid membrane shows strong ionic interaction between the Nafion matrix and the multifunctional POSS, resulting in increased glass transition temperature and thermal stability at very low loadings of S-POSS (1 %). The presence of S-POSS has also improved the proton conductivity especially at low humidities, where it shows a marked increase due to its confinement in the ionic domains and promotes water uptake by capillary condensation. In order to achieve anhydrous conductivity, the IL 1-butyl-3-methylimidazolium bis(trifluoromethylsulfonyl)imide (BMI-BTSI) was incorporated into these membranes to provide proton conduction in the absence of water. Although the incorporation of an IL shows a plasticizing effect on the Nafion membrane, the S-POSS composite membrane with an IL shows a higher modulus at high temperatures compared to Nafion 117 and a Nafion−IL membrane, with significantly higher proton conductivity (5 mS/cm at 150 °C with 20% IL). This shows the ability of the multifunctional POSS and IL to work symbiotically to achieve the desirable proton conductivity and mechanical properties of such membranes by enhancing the ionic interaction within the material.

KEYWORDS: high-temperature fuel cell membranes • organic−inorganic composite membranes • ionic liquids • polyhedral oligomeric silsesquioxanes

INTRODUCTION

One of the main challenges in the development of polymer electrolyte membrane fuel cells (PEMFCs) is to develop membrane materials with high operating temperatures above 100 °C because this significantly reduces catalyst poisoning and increases electrode kinetics (1−4). The current PEMFC relies on perfluorinated sulfonic acid membranes such as Nafion, which cannot operate at high temperature above 100 °C as dehydration occurs, resulting in the loss of proton conductivity. In order to increase the operating temperature of these membranes, a substitute charge carrier is required in place of water, such as room temperature ionic liquid (IL).

ILs are thermally stable and are well-known charge carriers with high conductivity. Under anhydrous conditions, they are able to act as charge carriers in absence of water (5−9). However, the use of ILs in membranes such as Nafion often leads to a lower elastic modulus of the resultant composite because of its plasticizing effect (8). On the contrary, the mechanical strength of a membrane matrix can be enhanced by adding an inorganic component, which can enhance the structure and ionic interaction within the material. Such additives would be able to improve the mechanical strength of the membrane and constrain dimensional changes due to swelling, resulting in better mechanical integrity and long-term stability. However, it is also important that the additive should not impede its performance at high temperatures. One such class of materials is polyhedral oligomeric silsesquioxanes (POSSs), which are multifunctional nanomaterials based on a silica cage with organic corner groups. The variety of organic functionalities that can be incorporated into their structures offer great versatility in their use in composites. They can be readily functionalized to provide optimum interaction between the inorganic component and the polymer matrix (10, 11). Such functionalized silsesquioxanes have been extensively studied with regards to their use in nanocomposites and catalysts (10, 12−15); however, there are relatively few investigations into their use in PEMFCs (16−18).

The use of hydrophilic inorganic particles in fuel cell membranes has been extensively studied, including the use of silica particles synthesized by sol−gel reactions (19−22). Such particles are known to assist water retention at higher temperature and improve the mechanical strength of the

* E-mail: Namita.Choudhury@unisa.edu.au.
Received for review January 9, 2009 and accepted April 25, 2009
[†] University of South Australia.
[‡] Australian Nuclear Science and Technology Organisation.
DOI: 10.1021/am900020w

Scheme 1. Sulfonation of OPS

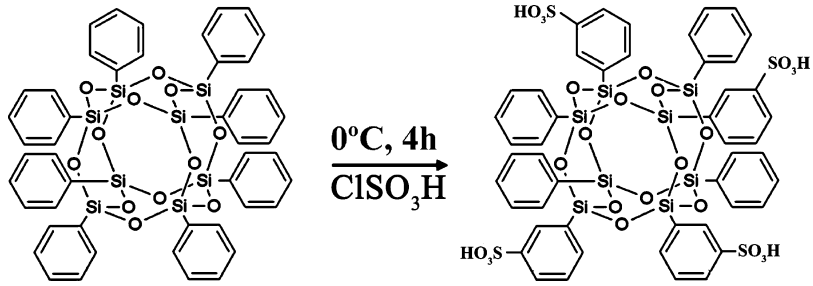

polymer. However, their nonconductive nature and their influence over the amount and behavior of water adsorbed in the membrane often result in a reduction of the proton conductivity. They are also often synthesized in situ within the membrane, and this may also result in a hydrophobic byproduct trapped in the membrane, further impeding proton transfer (19, 22, 23).

In previous studies, introducing sulfonic acid groups on the silica has been shown to enhance the proton conductivity of the resultant composite (24−28). POSS-type compounds can be readily functionalized with ionic functionalities, and because of their multifunctional nature, the POSS-type material has the ability to enhance the mechanical properties of the matrix polymer. This is advantageous in membranes utilizing ILs, where the IL has a plasticizing effect, thus reducing the mechanical strength of the membrane. Because a PEMFC would be required to operate under repeated on/off cycles involving large changes in temperatures, the membrane needs to be able to retain its original dimension and not deform or degrade under the operating conditions. In these membranes, the use of multifunctional POSS would improve the mechanical integrity of the composite membrane because the higher mechanical strength allows it to better resist deformation. It also has the potential to reduce leaching because it reinforces the polymer matrix and provides more interaction with the IL because the IL is typically bound to the polymer matrix by ion exchange.

In this paper, we describe the first investigation into a three-phase composite proton-conducting membrane material utilizing ionic liquid [1-butyl-3-methylimidazolium bis-(trifluoromethylsulfonyl)imide, BMI-BTSI] in a Nafion−sulfonated POSS (S-POSS) hybrid membrane. BMI-BTSI was chosen because of its commercial availability and compatibility with Nafion due to the butyl side chain and the perfluorinated counterion (8, 9).

Our hypothesis is that this combination will take advantage of the thermal stability and high conductivity of the IL and utilize S-POSS for structural reinforcement of the polymer matrix, achieving anhydrous conductivity and good mechanical integrity at high temperatures. The effect of S-POSS on the properties of Nafion and Nafion−IL membranes was investigated with respect to its structural, thermal, mechanical properties and proton conductivity.

EXPERIMENTAL SECTION

Materials. Octaphenyl polyhedral oligomeric silsesquioxane ($Ph_8Si_8O_{12}$, octaphenyl POSS, OPS) was purchased from Hybrid Plastics, Fountain Valley, CA. Chlorosulfonic acid was purchased from Aldrich and used as received. Nafion 117 films were purchased from Aldrich and prepared by refluxing in a 3% H_2O_2 solution for 2 h followed by refluxing in 0.5 M H_2SO_4 for 2 h, and the films were then rinsed by soaking in water at 70 °C. BMI-BTSI was purchased from Solvent Innovation (Cologne, Germany) and used as received.

Sulfonation of OPS. The sulfonic acid functionalized POSS was synthesized using sulfonation of OPS by chlorosulfonic acid according to Scheme 1. In a typical reaction, OPS (1 g, equivalent to 8 mmol phenyl groups) was suspended in chloroform (5 mL) and chlorosulfonic acid (4 mL, 42 mmol) was added dropwise at 0 °C. Upon addition of chlorosulfonic acid, the solution became clear with a pale-yellow tinge, and the solution was further stirred at 0 °C for 4 h under nitrogen. The solution was then poured onto crushed ice, and the precipitated material was filtered and dried under vacuum. The filtered solid was then washed several times with deionized water and dried under vacuum to yield a white, powdery solid (0.7 g, 68%). ^{1}H NMR (0.1 M NaOH in D_2O): δ_H (ppm) 8.04 (s, H ortho to both SO_3H and POSS), 7.85 (d, H ortho to SO_3H and para to POSS), 7.73 (d, H ortho to POSS and para to SO_3H), 7.52 (dd, H meta to both SO_3H and POSS) due to a sulfonated phenyl ring; peaks at δ_H7.39 (t, *p*-H), 7.55 (t, *m*-H), 7.8 (d, *o*-H) due to unfunctionalized phenyl rings. ^{13}C NMR (0.1 M NaOH in D_2O): δ_C (ppm) 141.1 (C−SO_3H), 137.3 (C−Si), 130.6, 129.0 (Ar−C) due to sulfonated phenyl rings; peaks at δ_C131.6, 130.3, 127.8, 125.1 (Ar−C) due to unfunctionalized phenyl rings. ^{29}Si NMR: δ_{Si} (ppm) 58 (Si−$ArSO_3H$), 68 (Si−Ar). FTIR: ν (cm^{-1}) 3320 (OH), 1699, 1377 (SO_3), 1140 (broad) (Si−O−Si); ν (cm^{-1}) 934 and 804 (*m*-CH).

Preparation of Hybrid Membrane. S-POSS was dissolved in a 0.1 M NaOH solution, and a Nafion 117 membrane (preswollen in water) was soaked in the solution for 5 days, after which the films were rinsed with deionized water and annealed at 100 °C overnight. The films were then soaked in 0.1 M HCl overnight to reacidify the sulfonic acid functionalities, after which they were rinsed with ultrapure water and dried at 30 °C under vacuum.

The hybrid membrane containing IL was prepared using a two-step layer-by-layer strategy. The hybrids (prepared in the first stage) were further soaked in a 10−30% solution of BMI-BTSI in methanol at 60 °C under reflux for 2 days, after which they were rinsed with methanol, wiped, and dried at 70 °C overnight. A higher concentration of IL in the soaking solution resulted in a greater uptake of IL with a maximum uptake of 32%. However, at such higher uptake, the IL leached out upon standing, and the maximum uptake that could be obtained without significant leaching upon standing was 20%.

Spectroscopic Analysis. Photoacoustic Fourier transform infrared spectroscopy (PA-FTIR) was performed on a Nicolet Magna-IR 750 spectrometer equipped with an MTEC model 300 photoacoustic cell under a helium purge with carbon black as the reference. ^{1}H NMR spectroscopy was done on a Varian 600 MHz NMR spectrometer. ^{13}C NMR was performed using a

Bruker 350 MHz NMR spectrometer. ^{29}Si NMR spectroscopy was performed on a Varian 300 MHz NMR spectrometer. Chromium(III) acetylacetonate was used as a spin-relaxation agent to improve the sensitivity. For all of the NMR analyses, S-POSS was dissolved in a 0.1 M solution of NaOH in D_2O.

Morphological Study. Small-angle X-ray scattering (SAXS) data were obtained at various temperatures using thin films of samples and a S3-MICRO SAXS/wide-angle X-ray scattering (WAXS) instrument (HECUS GmbH, Graz, Austria), which consists of a GeniX microfocus X-ray source (Xenocs, Grenoble, France; sealed Cu Kα source, power 50 W, brilliance ~10^9 photons/s/mm^2/mrad^2/% bandwidth) integrated with FOX2D single-bounce multilayer optics, providing a point-focusing beam delivery system with low divergence (<1 mrad). The sample was loaded into a 2-mm-diameter quartz capillary (Charles Supper Co., Natick, MA) and mounted in the single-position heater block. Simultaneous SAXS/WAXS data were collected as a function of the temperature using the instrument control software. The instrument is equipped with two one-dimensional (1D) position-sensitive detectors (HECUS 1D-PSD-50 M system); each detector is 50 mm long (spatial resolution 54 μm/channel, 1024 channels) and covers the SAXS Q range ($0.003\ Å^{-1} < Q < 0.6\ Å^{-1}$) and the WAXS Q range ($1.2\ Å^{-1} < Q < 1.9\ Å^{-1}$).

Thermal Analysis. Thermogravimetric analysis (TGA) was carried out on a TGA 2950 thermal analyzer (TA Instruments, New Castle, DE). The samples were first dried overnight at 70 °C to remove water, and the experiment was performed on approximately 10 mg of the sample under nitrogen with a temperature ramp of 10 °C/min up to 850 °C, upon which the gas was switched to oxygen and the temperature ramped up to 900 °C. For water uptake experiments, the samples were soaked in water overnight and carefully wiped to remove the surface water before the experiments were performed. Dynamic mechanical analysis (DMA) was performed on a DMA 2980 (TA Instruments, New Castle, DE) in tension mode on films with a typical dimension of 20 × 5 × 0.2 mm. For the analysis, the samples were dried in an oven at 80 °C before use and the temperature was ramped at 3 °C/min at a frequency of 1 Hz from 30 °C up to 250 °C. The samples were subjected to a static force of 0.05 N and an oscillation amplitude of 10 μm. Differential scanning calorimetry (DSC) was done on a TA 2920 DSC (TA Instruments, New Castle, DE) at a heating rate of 10 °C/min under nitrogen. The samples were dried in an oven at 70 °C for 4 h prior to analysis.

Ion-Exchange Capacity (IEC). Because the synthesized S-POSS was soluble in aqueous alkaline solutions, the IEC was measured through backtitration of NaOH rather than direct ion exchange with a salt. The samples were soaked in 0.05 M NaOH overnight after sonication for 1 h (after which it is assumed that all of the protons on the sulfonic acid have been neutralized), and the solution was then titrated with standardized 0.05 M HCl using a methyl red indicator. The IEC was obtained based on the difference in the volume of HCl required to neutralize the solution compared to a blank with no sample present ($V_{blank} - V_{sample}$) and was calculated according to eq 1.

$$\text{IEC (mmol/g)} = \frac{[(V_{blank} - V_{sample})\ (\text{mL})]M_{HCl}}{\text{mass}_{polymer}\ (\text{g})} \quad (1)$$

The number of water molecules per ionic site ($[H_2O]/[SO_3^-]$, λ) was then calculated with eq 2

$$\lambda = \frac{\text{water uptake (\%)} \times 10}{18\text{IEC (mmol/g)}} \quad (2)$$

Proton Conductivity. In-plane proton conductivity measurements were performed by alternating-current impedance using a Solartron 1260A electrochemical analyzer in a two-electrode setup. The films were cut into a 5 mm × 20 mm strip, and measurements were performed in an ESPEC 2930 controlled humidity chamber. The impedance of the film as then calculated with eq 3.

$$\sigma = \frac{l}{Rhw} \quad (3)$$

where l is the distance (cm) between the two platinum electrodes, h and w are the thickness (cm) and width (cm) of the membrane, respectively, and R (Ω) is the resistance of the membrane obtained from the complex impedance plot. The measurements were done in duplicate with an error margin of 5%.

Stability Testing. The stability of the IL membranes was examined by immersing them in water for 3 days at 70 °C and measuring the change in mass after drying, which is assumed to correspond to the loss of IL due to the fact that the conditions used do not result in degradation of Nafion. For the hybrid membranes without IL, the stability was tested by comparing the amount of residue obtained from TGA before and after leaching in water for 5 days at 70 °C.

RESULTS AND DISCUSSION

Characterization of S-POSS and the Hybrid Membrane. The synthesis of S-POSS was performed in a concentrated chlorosulfonic acid solution. Low temperature was necessary to control the reaction because sulfonation at room temperature or higher resulted in a very low yield. Previous studies on the sulfonation of poly(phenylsilsesquioxane) (29) or OPS (30) were performed in chloroform using a dilute chlorosulfonic acid−chloroform mixture, but in this investigation, it resulted in a low degree of sulfonation, which was reflected by a low IEC of less than 0.5 mequiv/g. Sulfonation with neat chlorosulfonic acid such as the method used by Hartmann-Thompson et al. on OPS (17) resulted in a water-soluble product, indicating a very high degree of sulfonation. Because the use of such highly soluble species may pose long-term stability issues (the soluble S-POSS may leach out of the membrane), we chose to use a partially sulfonated material, which can be readily incorporated into PEMs by the infiltration method in an alkaline solution but would be retained within the membrane after it was reacidified. The extent of sulfonation depends on the amount of chlorosulfonic acid added, and when 3−6 mL of concentrated chlorosulfonic acid in chloroform was used per gram of OPS, the resultant materials show an IEC of around 2−2.5 mequiv/g, which corresponds to approximately 40% sulfonation of the phenyl rings. A typical procedure utilizing 5 mL of chlorosulfonic acid to sulfonate 1 g of OPS resulted in a product with an IEC of 2.28, corresponding to 38% sulfonation. The use of low temperature was required to achieve better control of the reaction because the reaction is exothermic, and a previous study (29) reported that ring cleavage may occur during sulfonation. When an excess of chlorosulfonic acid or a longer reaction time was used, the amount of sulfonated OPS precipitated decreases as the amount of water-soluble, highly sulfonated species in-

creases. In contrast, S-POSS with sulfonation of around 50% or less is not readily soluble in water (because it was precipitated in a cold, acidic solution) but dissolves in aqueous alkaline solutions.

The sulfonation of POSS was confirmed by PA-FTIR and NMR spectroscopy. The PA-FTIR spectrum of S-POSS shows a strong, broad peak in the region 3000−3500 cm^{-1} resulting from hydrogen-bonded OH groups due to the presence of sulfonic acids compared to the original material, as well as peaks at 1377 and 1080 cm^{-1} due to SO_3 assymmetric and symmetric stretching, respectively, 1590 and 1470 cm^{-1} (aromatic C−C ring stretch), 934 and 804 cm^{-1} (out-of-plane bending for a meta-substituted aromatic ring), as well as changes in the weak aromatic overtones around 1600−1800 cm^{-1} due to the meta substitution. The peaks at 1418 cm^{-1} (Si−Ar) and 1109 cm^{-1} (broad, Si−O−Si) are due to POSS. This is supported by ^{1}H NMR spectroscopy, which shows seven peaks in the aromatic region due to unfunctionalized phenyl rings (three peaks) and meta-sulfonated phenyl rings (four peaks), with a peak at 8.04 ppm due to the protons ortho to the sulfonic acid group and POSS. ^{13}C NMR of S-POSS also shows a peak at 141.1 ppm due to the carbon attached to the sulfonic acid functionality, with an upfield shift on the carbon atoms of the sulfonated phenyl rings (29). The ^{29}Si NMR spectrum of S-POSS shows two multiplets at −58 and −68 ppm, which is attributed to silicon attached to the sulfonated and unsulfonated aromatic rings, respectively. However, peak area analysis from ^{1}H NMR indicates a sulfonation level >40%, which is higher than what is expected based on the IEC, and as such, it is likely that some ring cleavage (29) has occurred, lowering the number of unfunctionalized aromatic rings present in S-POSS.

Impregnation of the Nafion Membrane with S-POSS and IL. Because of the hydrophobic nature of the IL and the hydrophilic nature of S-POSS, we adopted a two-step layer-by-layer strategy to incorporate both components into a PEM. This was done by infiltration of S-POSS into the Nafion membrane to create a hybrid organic−inorganic membrane followed by impregnation of the hybrid membrane with the hydrophobic IL. The Nafion−S-POSS hybrid membrane prepared by soaking preswollen Nafion membranes in an aqueous solution of S-POSS remains clear, and TGA shows an inorganic content of around 1%, which is predominantly made of Si−O from the POSS core, as evidenced by scanning electron microscopy−energy-dispersive X-ray (EDX) analysis. Although the amount of S-POSS incorporated is low, this is desirable because the previous study on sol−gel-synthesized silica composites indicated that a large inorganic content may be detrimental to the proton conductivity because of aggregation and reduction of water uptake. Yen et al. (22) studied sulfonated silica−Nafion composites with 0.3−1.2% inorganic content and found that the conductivity decreased above 0.6% silica content.

Because the soaking was performed in an aqueous alkaline solution (and thus the hybrid was obtained in its sodium salt form), the membrane was reacidified by soaking in HCl. However, very little inorganic content was observed if the membrane was reacidifed without prior annealing. This is ascribed to the leaching of S-POSS. In contrast, samples that were annealed at higher temperatures above 80 °C before reprotonation did not display significant leaching of the inorganic phase. This observation indicates that annealing of the sample has confined S-POSS within the Nafion matrix.

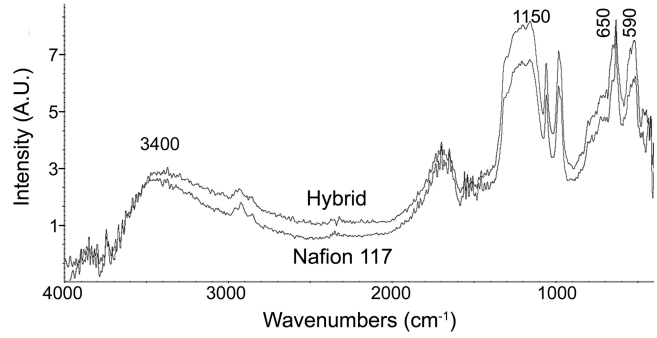

FIGURE 1. PA-FTIR spectra of the hybrid material and Nafion 117.

A comparison of the PA-FTIR spectra of Nafion and the hybrid material in Figure 1 shows a broadening of the sulfonic acid peaks at 1150, 650, and 590 cm^{-1} in the Nafion−S-POSS hybrid compared to blank Nafion. There is also a marginal increase and broadening of the peak at 3400 cm^{-1} due to the −OH groups of the sulfonic acids. The differences observed are marginal because of the low amount of S-POSS present, and the broadening of the −OH peak indicates that S-POSS is interacting with the polymer matrix through increased hydrogen bonding via the protons of the sulfonic acid groups.

The addition of S-POSS also resulted in a marginal increase in the IEC, with the hybrid showing an IEC value of 1.06 compared to 0.95 for Nafion. This increase is marginally higher than expected because of the low concentration of S-POSS incorporated but is still within the error margin of the expected theoretical increase. The incorporation of S-POSS also reduces the free volume of the membrane. Under equilibrium condition at room temperature, the hybrid material shows a 2% reduction (from 14% to 12%) in maximum water uptake compared to pure Nafion. Because the percentage reduction in water uptake (2%) is greater than the percentage of S-POSS incorporated (1%), this also indicates that interaction of the S-POSS and the matrix has constrained the membrane, reducing the swelling.

In order to enhance its anhydrous conductivity, IL is incorporated because it is able to act as a charge carrier at high temperature. The IL chosen for this study was 1-butyl-3-methylimidazolium bis(trifluoromethylsulfonyl)imide (BMI-BTSI), which possesses a fluorinated counterion and has good compatibility with Nafion. The previous study using this IL (8) has shown good high-temperature conductivity as well as mechanical properties at low uptake, comparable to wet Nafion. Figure 2 shows the PA-FTIR spectrum of the hybrid membrane containing the IL. The spectrum shows several additional peaks around 3000 and 1500 cm^{-1} due to C−C bonds in the imidazole ring and alkyl side chain of the IL.

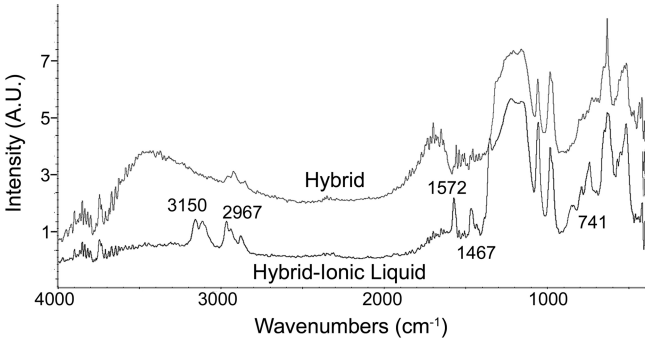

FIGURE 2. PA-FTIR spectra of the ionic-liquid containing membrane compared to the hybrid material.

However, the peak due to the hydroxyl groups at 3400 cm^{-1} (from the sulfonic acid functionalities of Nafion) has been suppressed when IL is present, indicating that the acidic protons have been replaced by the imidazolium cation. This observation confirms that the IL takes part in ion exchange with the polymer matrix, where the imidazolium cations have replaced the protons from the sulfonic acid sites. This is beneficial because ion exchange would result in ionic bonding between the sulfonate anion and the imidazolium cation, and as such, some of the IL is held or bound in the membrane by interactions similar to the bound water in hydrated membranes, which are held by strong hydrogen bonding. Furthermore, this shows that the IL is able to promote proton dissociation in the same way that water does, which is necessary for good proton conductivity.

In order to estimate the stability of these membranes, they were subjected to leaching by immersion in water. First, the Nafion–S-POSS hybrid was tested in the absence of ILs. TGA performed after leaching showed that the amount of inorganics has been reduced by 10% of the original content (a reduction from 1% to 0.9%). This results in only a slight reduction in the proton conductivity, with the hybrid membrane showing proton conductivities of 103 ± 3 mS/cm [at 80 °C and 100% realtive humidity (RH)] after leaching compared to 110 ± 5 mS/cm before leaching. When the sample was subjected to several days of vigorous reflux at 100 °C, a greater loss of the inorganic content was observed but the hybrid membrane still retained ~50% of its original inorganic content. This result indicates that S-POSS is strongly interacting with the Nafion matrix and that annealing of the sample has helped to improve the stability of the hybrid. The IL membrane was then examined under similar conditions, and for the membrane containing 20% IL only, a small mass loss (5–10% of the original) was observed after soaking in water at 70 °C for 3 days. Thus, the hydrophobic nature of the IL, in addition to its ion-exchange reaction with Nafion, confines the IL within the membrane and minimizes leaching after immersion in water. Furthermore, there is no loss of S-POSS observed in the hybrid IL membranes, indicating that the ionic interaction between S-POSS and the IL within the ionic domains of Nafion is able to confine S-POSS within the membrane.

Structural Analysis. Transmission electron microscopy (TEM) analysis of the cross section of the Nafion–S-POSS hybrid is shown in Figure 3. Both uniform distribution

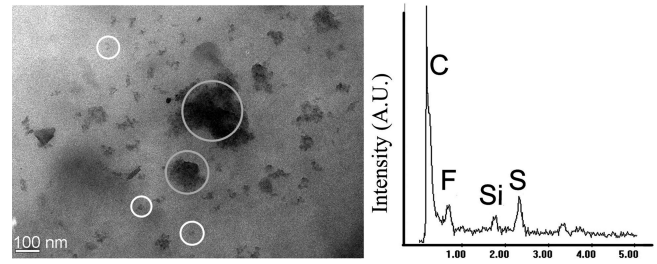

FIGURE 3. Aggregation of S-POSS observed in a cross-sectional TEM image of the dry Nafion–S-POSS hybrid membrane showing small (white circle) and large (gray circle) aggregates and EDX analysis of the aggregates.

and aggregation of S-POSS are observed in the material with clusters of varying sizes. The majority of the clusters are below 20 nm in size, with some larger aggregates present in the material that result from the aggregation of smaller clusters when the material is dried. EDX analysis shows that S-POSS resides mainly in the aggregates, although the analysis shows higher carbon and sulfur contents due to the sulfonated aromatic rings in S-POSS. EDX of the aggregates also reveals the presence of fluorine, which is due to the perfluorinated sulfonic acid side chain of Nafion being present in the ionic domains where these aggregates reside. Thus, S-POSS is interacting with and is not completely separated from the Nafion. This aggregation may have occurred during annealing because of the phase separation inherent in Nafion, with S-POSS aggregating within the hydrophilic domains. These aggregates are found inside the material and not just near the surface, indicating incorporation of S-POSS into the Nafion membrane. The aggregation most likely occurs during post-treatment and not during impregnation of the membrane.

This phase-separated morphology observed in Nafion and the hybrid has also been studied using SAXS. Previous SAXS examinations on Nafion (31–34) consistently showed characteristic profiles of these membranes with three prominent features: an ionomer peak at $q \sim 0.2$ $Å^{-1}$, which is attributed to the aggregation of ionic groups to form ionic domains (local order), a broad peak at $q \sim 0.04$ $Å^{-1}$, which is associated with crystallites in the fluorocarbon matrix, and an upturn in the intensity at very small angles ($q < 0.01$ $Å^{-1}$), which is related to large-scale heterogeneities (long-range order). SAXS was performed in the q range 0.008–0.6 $Å^{-1}$ to probe the structures of Nafion hybrids at the molecular length scale. Figure 4 shows the SAXS profiles for unmodified Nafion, a Nafion–S-POSS hybrid, and a Nafion–S-POSS–IL composite. The SAXS profile of the unmodified Nafion membrane clearly shows the ionomer peak centered around $q \sim 0.22$ $Å^{-1}$, a broad peak due to the crystalline region at around 0.05 $Å^{-1}$, and an upturn in the intensity at $q < 0.02$ $Å^{-1}$. The ionomer peak at $q = 0.22$ $Å^{-1}$ in unmodified Nafion corresponds to a d spacing of approximately 28.6 Å. The SAXS profile of the Nafion–S-POSS hybrid is very similar to that of the unmodified Nafion; however, there is a marginal decrease in the intensity that is more pronounced at low q values along with a slight shift in the ionomer peak. Similar profiles between unmodified Nafion and the hybrid can be attributed to the low inorganic content in the hybrid

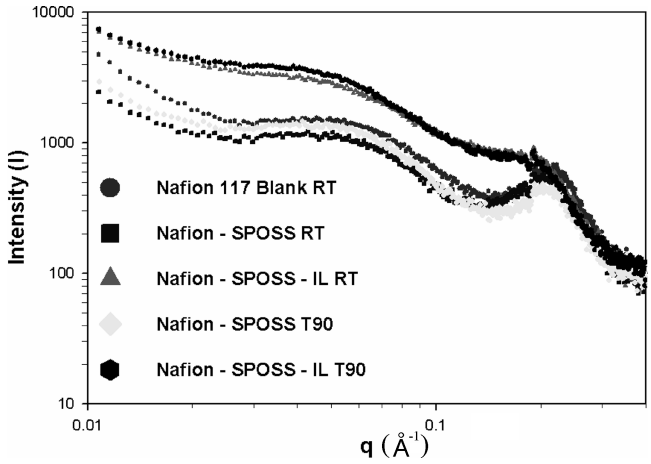

FIGURE 4. SAXS spectra of unmodified Nafion, a Nafion–S-POSS hybrid, and a Nafion–S-POSS–IL composite membrane.

membrane (only 1 %). The marginal decrease in the intensity and shift of the ionomer peak in the hybrid membrane indicates that the size of the clusters in Nafion has increased, resulting in a decrease in the number of ionic domains with increased size due to incorporation of S-POSS. The presence of S-POSS has very little effect on the hydrophobic matrix because there is little change in the broad peak related to crystalline regions. The ionomer peak has shifted from 0.22 Å^{-1} in the unmodified Nafion to 0.2 Å^{-1} in the hybrid, which corresponds to a *d* spacing of 31.4 Å. The presence of a small amount of S-POSS has increased the intercluster distance by 2.8 Å. In the case of the Nafion–IL membrane, there are considerable changes in the SAXS profile. The ionomer peak has shifted to $q = 0.186$ Å^{-1} and has become much broader in shape with increased intensity, which corresponds to a *d* spacing of 33.6 Å. The incorporation of IL into the hybrid membrane has increased the intercluster distance between ionic domains. There is a significant increase in the intensity of the crystalline peak, which has also slightly shifted, indicating the interaction of IL with both ionic domains and the fluorocarbon matrix of Nafion. The hypothesis is that the hydrophilic cation is directed toward the ionic domains and, hence, the increase in spacing between these clusters. The fluoro-containing anion, which is more hydrophobic in nature, is more compatible with the hydrophobic matrix. The shift in the crystalline peak suggests that the crystallites have increased in size because of the presence of the anion of the IL. Figure 4 also shows profiles for the hybrid and the hybrid with IL at 90 °C. The Nafion hybrid at 90 °C shows a decreased intensity in the ionomer peak but an increased intensity in the crystalline peak. As the temperature is increased, the number of ionic clusters decreases but the number of crystalline regions increases. In the case of the hybrid with IL at 90 °C, there is no change in the ionomer peak but there is a marginal increase in the intensity of the crystalline peak. These results indicate that there is a change in the structures of both ionic cluster and crystallites with an increase in temperature. The IL is likely to be partially incorporated into the fluorocarbon as well as the ionic clusters of Nafion. This would result in the partial homogenization of the membrane, which is consistent with the

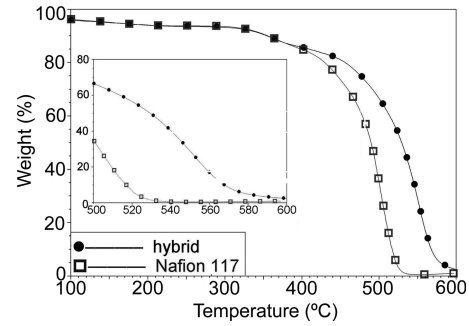

FIGURE 5. TGA comparison of Nafion 117 and the Nafion–POSS hybrid membranes.

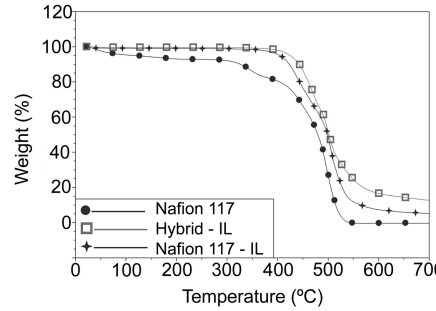

FIGURE 6. TGA of the IL-containing membranes compared to Nafion.

SAXS results. Bennett et al. (35) have also reported similar observation when they incorporated the IL 1-ethyl-3-methylimidazolium bis(trifluoromethanesulfonyl)imide into Nafion. They also indicate that the structure of Nafion in a Nafion–IL composite membrane is strongly dependent on the structure and properties of the IL.

Thermal and Mechanical Analysis. The thermal stability of the hybrid membrane was investigated using TGA. Figure 5 shows a comparison between Nafion and the hybrid membrane, both of which show two-step decomposition with a marginal loss of mass at around 260 °C due to the loss of a sulfonic acid group and a main degradation around 420–500 °C due to the degradation of the polymer. There is little difference between the two materials at 260 °C (where desulfonation occurs) due to similar IEC of the two materials (and, hence, similar sulfonic acid content). However, the onset of the main thermal degradation of the material has shifted by 20 °C from 420 to 440 °C in the hybrid, indicating an increase in the thermal stability of the polymer. The inset in Figure 5 shows an expanded view of the region between 500 and 600 °C, in which the hybrid material displays a small mass loss at 500–530 °C. This is attributed to the presence of aromatic rings on the OPS, which would result in a higher amount of char. The hybrid membrane also shows a greater amount of residue at 600 °C due to the presence of silica.

When IL was incorporated into the membrane, the TGA result showed a significant increase in the thermal stability. As can be seen in Figure 6, there is no mass loss around 260 °C associated with desulfonation in the IL-containing membranes. A similar result was observed when the TGA experiment was repeated with the sodium salt form of Nafion, which supports our previous observation that the IL has

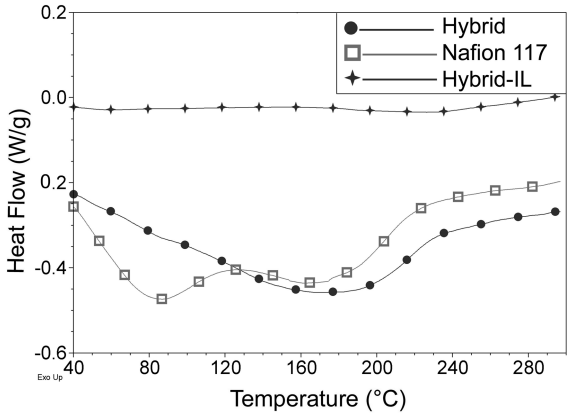

FIGURE 7. DSC thermogram of Nafion 117, the hybrid material, and the Nafion−S-POSS−IL membrane.

entered into an ion-exchange reaction with the sulfonic acid functionalities (PA-FTIR spectrum in Figure 2), preventing desulfonation at higher temperatures. This interaction will also be advantageous towards the long-term stability of the membrane because it will prevent desulfonation and degradation of the Nafion. The addition of S-POSS has further increased the thermal stability of the material, with an increase in the onset of thermal degradation attributed to increased ionic interaction in the material. This ion-exchange interaction between the IL and the polymer was also investigated by DSC. Figure 7 shows the DSC thermogram of Nafion 117, a hybrid membrane, and the IL-containing membranes. Nafion shows an endothermic peak at around 90 °C and another endothermic peak at around 170 °C. The first peak at 90 °C is attributed to an ionic cluster transition (36−38) and is known to be affected by the nature of the counterion and also hydration. In the hybrid, the first peak was completely suppressed, indicating that S-POSS has interacted with the ionic clusters. This observation supports what has been previously observed in SAXS (Figure 4), where the spectrum of the hybrid shows only a slight change in both the ionomer and crystalline peaks at 90 °C and is attributed to the order−disorder transition of the ionic cluster. The second peak at 170 °C is related to the T_g of Nafion. In the hybrid, this peak has been shifted to 180 °C in Nafion−IL. Thus, it appears that the presence of S-POSS has broadened the peak, indicating ionic interactions; however, the glass transition temperature of the polymer has shifted because of the reinforcement effect caused by the strong interfacial interaction between S-POSS and Nafion. When IL is present, both phase transitions weaken significantly because of the effect of the larger butylimidazolium cation replacing the protons on the sulfonic acids, resulting in a more disordered, amorphous material with no observable phase transition.

In order to investigate the effect of S-POSS or ILs on the mechanical properties of Nafion, DMA was performed on the membranes. The tan δ curves of Nafion 117 and the hybrid membrane obtained from DMA are shown in Figure 8. It shows that the peak indicative of ionic cluster transition T_c has broadened and shifted from 119 to 127 °C. This broadening and shift of the tan δ peak indicates that the

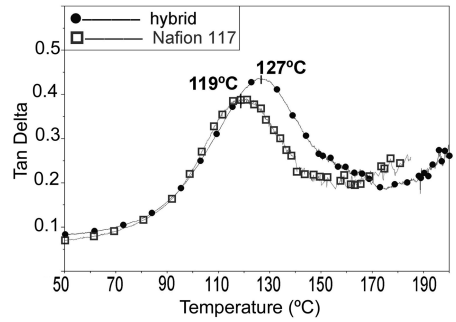

FIGURE 8. DMA showing the shift in T_g in the tan δ curve for the Nafion−S-POSS hybrid compared to Nafion.

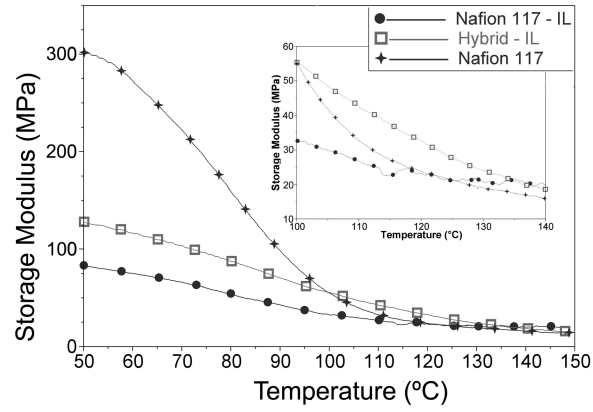

FIGURE 9. DMA of the Nafion−S-POSS−IL composite membrane material and the Nafion−IL membrane (inset: an enlargement of the region between 100 and 140 °C).

incorporation of S-POSS has affected the ionic clusters in Nafion, broadening the peak as a result of the strong ionic interaction within the ionic domains because of the sulfonic acid groups on S-POSS. Because this is achieved with a very low loading of S-POSS, it also indicates strong interactions between the polymer and S-POSS due to its small size and multifunctional nature.

The addition of IL strongly affects the modulus of the membrane, and the storage modulus curves of Nafion, Nafion−IL, and the Nafion−S-POSS−IL composite membrane are shown in Figure 9. Near room temperature the IL-containing membrane has a significantly lower modulus of ∼100 MPa compared to dry Nafion, which has a modulus of ∼300 MPa. The storage modulus of the membranes decreased with temperature, and this decrease was more evident in Nafion 117, where the modulus decreased sharply until it became very similar to that of the Nafion−IL membrane above 120 °C (the T_c of Nafion observed in DMA; Figure 7). The tan δ curve shown in Figure 10 also shows that when IL is incorporated, the tan δ peak around the expected T_c of Nafion has become significantly broader and weaker, indicating different degrees of interaction within the material. The broadening of the tan δ peak and the lowering of the modulus obtained for IL systems show the plasticizing effect of the IL, which increases the flexibility of the membrane, resulting in an amorphous, elastic material with no well-defined transition.

The S-POSS-containing hybrid membrane is similarly affected because of the presence of the IL, showing a

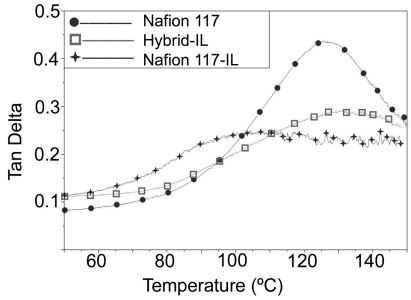

FIGURE 10. tan δ curves of the Nafion−S-POSS−IL composite membrane material and the Nafion−IL membrane.

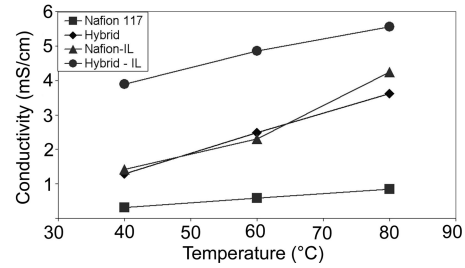

FIGURE 11. Proton conductivity comparison at 20% RH and varying temperatures.

significant reduction in the modulus. However, the Nafion−S-POSS−IL composite membrane shows an increased modulus of 120 MPa compared to that of the Nafion−IL membrane (100 MPa). Furthermore, as can be seen from the inset in Figure 9, at around 120 °C the hybrid IL membrane shows a greater modulus of 32 MPa compared to both Nafion 117 and Nafion−IL membranes, both of which show similar modulus of 23 MPa around this temperature. This is attributed to the increased ionic interaction in the membrane when S-POSS is present, which enhances the mechanical integrity of the composite above the T_c of Nafion. This observation is of interest because an operating temperature of 120 °C would be considered sufficiently high to confer the benefits of high-temperature operation (39), and at this temperature, the hybrid material should exhibit significant improvement in mechanical stability compared to Nafion.

Proton Conductivity. At 100% RH and 80 °C, the hybrid material shows a proton conductivity of 110 ± 5 mS/cm, compared to 90 ± 4 mS/cm for Nafion 117. Previous studies (20, 22) on a sol−gel-synthesized, sulfonated silica−Nafion composite have also reported similar increases in conductivity for composites with 1−4% silica content. Because of the low amount of S-POSS involved, it is likely that the increase in proton conductivity is due to a combination of effects, namely, the increased availability of sulfonic acid groups within the ionic channels and the structural effect of S-POSS constraining the ionic channels within the Nafion. Because it has been previously observed that the proton conductivity tends to increase as the particle size decreases (40), the small size of S-POSS enables the enhancement of proton conductivity using very low loadings due to their large effective surface area. Even though some aggregation seems to occur based on the TEM image, this has been observed under dry conditions, and such aggregation is likely to be disrupted under hydrated conditions, leading to smaller-sized clusters than what have been observed in the dry sample.

Despite the higher conductivity, the hybrid material reveals a lower water uptake of 12% compared to 14% for Nafion 117. This uptake translates to a λ value (number of water molecules per sulfonic acid group) of 8.2 for Nafion and 6.4 for the hybrid material. The previous study by Paddison (41) shows that partial dissociation of protons will occur at λ of less than 3 and full dissociation at λ of 6. Because both materials still possess greater λ than this threshold, the reduction in water uptake is unlikely to affect the conductivity of the hybrid membrane. Some earlier works (20, 22) on a sol−gel-synthesized, sulfonated silica−Nafion composite also utilized the solution-casting method in their membrane synthesis, resulting in much higher water uptake up to 80%, which would affect the mechanical integrity of the hydrated film. High water uptake may result in large dimensional changes and the loss of mechanical strength.

Under low-humidity conditions, the proton conductivities of both Nafion and the hybrid material are significantly lower because both materials rely on water for proton transport. However, as shown in Figure 11, at 20% RH the hybrid material shows a greater increase in the proton conductivity with temperature compared to that of Nafion. On the basis of TEM images, S-POSS is present in some locations as aggregates that may not be optimal for charge transfer. Despite this, the increase of the conductivity of the material under hydration implies that aggregation of S-POSS is reversible when the membrane is hydrated. It is likely that the aggregates are disrupted under hydration, and the increased dispersion and availability of sulfonic acid groups within the hydrophilic domains resulted in increased proton conductivity.

The increased conductivity values at low humidity also suggest that the Nafion−S-POSS hybrid has better water retention than Nafion. Water desorption measurements by TGA show that the hybrid has a diffusion coefficient of 9×10^{-7} cm^2/s, which is 31% lower than the value obtained for Nafion under the same conditions (1.3×10^{-6} cm^2/s). Furthermore, at 20% RH, the hybrid material has higher water content (3%) compared to Nafion (1.6%). This may seem counterintuitive as Nafion uptakes more water at equilibrium swollen condition, but it has been previously postulated that in PEM smaller domains of less than 5 nm are more effective at extracting water from the surrounding atmosphere because of capillary condensation (42). Although our TEM analysis shows that the POSS aggregates are around 10−20 nm in size, there are also many smaller aggregates present, which at low humidity increases the water uptake in a similar fashion by confining the size of the hydrophilic domains through ionic cross-linking, resulting in increased water content under those conditions. In terms of the number of water molecules per sulfonic acid, this means that, at 20% RH, Nafion has a λ of 0.9 while the hybrid has a λ of 1.6. Although this value is still lower than the threshold required for proton dissociation (and thus for the vehicular mechanism of proton transport), it indicates

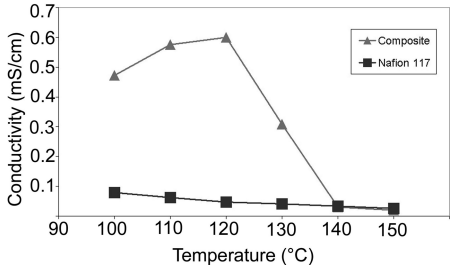

FIGURE 12. Proton conductivity under high-temperature, anhydrous conditions of the hybrid material compared to Nafion.

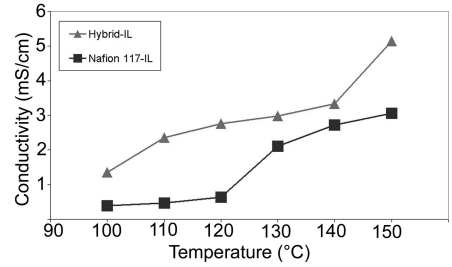

FIGURE 13. Proton conductivity under high-temperature, anhydrous conditions of the Nafion–S-POSS–IL composite membrane material and the Nafion–IL membrane.

that there are significantly greater amounts of water available in the hybrid membrane, which would assist in proton hopping between the ionic domains.

The incorporation of S-POSS has also increased the proton conductivity of the material under anhydrous conditions (above 100 °C). As can be seen in Figure 12, the hybrid material shows higher proton conductivity values of up to 0.6 mS/cm compared to Nafion 117. In contrast, the proton conductivity of Nafion decreases with temperature, while the conductivity of the Nafion–S-POSS hybrid increases up to 120 °C, after which the conductivity decreases. Under anhydrous conditions, the conductivity mechanism would be predominantly reliant on proton hopping between acidic sites, and the increased conductivity indicates that the incorporation of S-POSS is able to improve the interconnectivity between the ionic domains. However, the drop beyond T_c of the material indicates that the increase in conductivity may be partially attributed to structural factors, with S-POSS acting as intermediates for proton hopping between ionic clusters. Hickner and Pivovar (43) noted that the morphological structure, and in turn the conductivity, of PEM is highly dependent on the size and shape of the ionic domains, and it is known that above the transition temperature the ionic clusters become very mobile and the clustered structure collapses (2). In the case of the hybrid membrane, S-POSS enables one to maintain an interconnected, clustered morphology beneficial for proton conduction between 100 and 120 °C. However, above 120 °C, the ionic channels collapse because of softening of the Nafion matrix, thus reducing the conductivity of the material.

When IL was incorporated into the membranes, the low-humidity conductivities of both Nafion and the hybrid increased significantly. In Figure 11, the conductivity of the Nafion–IL membrane at 20% RH shows a significant increase compared to Nafion. However, the conductivity value obtained is similar to that of the Nafion–S-POSS hybrid (without any IL). The Nafion–S-POSS–IL composite shows the best conductivity at low humidity, indicating that the addition of S-POSS and IL has a cumulative effect on the conductivity of Nafion. This is attributed to the increased absorption of water vapor in the S-POSS-containing membrane because a small amount of water has been previously observed to increase the conductivity of IL membranes (44).

Under anhydrous conditions, both the Nafion–IL membrane and the Nafion–S-POSS–IL composite membrane show significant increases in conductivity with temperature. As can be seen in Figure 13, the conductivity of the Nafion–IL membrane shows a significant increase just beyond its T_c. Comparatively, the proton conductivity of the Nafion–S-POSS–IL composite membrane increased almost linearly with temperature. Previous studies (35, 41) have shown that conductivity in PEM occurs through a combination of proton hopping between ionic sites and vehicular transport by the liquid charge carrier (such as water or IL). In the case of the Nafion–IL membrane, as the temperature is increased above its T_c, the matrix possesses greater flexibility. This allows better mobility of IL within the membrane, enhancing the vehicular transport of protons by the IL and thus its conductivity. In contrast, the comparative linearity in the Nafion–S-POSS–IL composite membrane indicates that the presence of S-POSS helps maintain the ionic channel structure at those temperatures, and the conductivity increases linearly as the mobility of the charge carrier increases. Because this increase in conductivity is also greater than the increase due to S-POSS alone (in the absence of IL), it shows that the beneficial effect of S-POSS is not due to extra sulfonic acid groups alone. As such, it is most likely a combination of an increased number of charge carriers and better interconnection between ionic domains, with S-POSS acting as a bridge for proton transfer between acidic sites on the Nafion matrix.

Schmidt et al. (8), who studied similar ILs in Nafion membranes, have reported values of around 1 mS/cm at 120 °C, with the highest value quoted around 5 mS/cm at 150 °C. However, this was achieved with up to 32 wt % of the IL, and the value of 2.8 mS/cm obtained for the Nafion–IL membrane in this study reflected the lower uptake used (20%). Despite the lower uptake, our Nafion–S-POSS–IL composite membrane was able to perform equally or better than the literature values, with conductivities of 5 mS/cm at 150 °C and 2.6 mS/cm at 120 °C. Also, its anhydrous conductivity was significantly higher than the value obtained for Nafion–IL membranes at 120 °C, which would approximate the maximum operating temperature for these membranes because the long-term stability of the membrane may be compromised above these temperatures.

CONCLUSION

In this study, we have demonstrated that S-POSS can be synthesized by direct sulfonation of OPS and can be incorporated into Nafion membranes using the facile layer-by-layer technique. The multifunctional nature and small size of S-POSS enable strong interaction with the Nafion matrix,

as confirmed from FTIR and thermal analyses. It is, therefore, able to act as a reinforcing agent, improving the thermal stability and mechanical properties of the membrane. This structural reinforcement, coupled with the sulfonic acid functionalities present on S-POSS, also helps to improve the proton conductivity because S-POSS resides within the ionic domains of Nafion, providing extra charge carriers, and helps to constrain the ionic microstructure. It also improves the ability of the membrane to uptake water under low humidities as well as allowing greater anhydrous conductivity. The addition of IL to the Nafion−S-POSS hybrid membrane increased the conductivity of the membranes under both anhydrous and low-humidity conditions. The incorporation of S-POSS in such IL membranes improved the mechanical properties and conductivity at high temperatures, with the greatest increase in the performance found at 120 °C. At this temperature, the Nafion−S-POSS−IL composite membrane shows a significantly greater proton conductivity and modulus compared to those of both Nafion and the Nafion−IL membrane, exhibiting a cumulative effect from the addition of S-POSS and IL. This work demonstrates the potential of multifunctional POSS-based materials for the structural reinforcement of supported liquid membranes.

Acknowledgment. The authors thank the Australian Research Council (ARC) for financial support through the "Discovery Projects" funding and the Australian Institute of Nuclear Science and Engineering (AINSE) for funding of the SAXS work through an AINSE award.

Supporting Information Available: Detail elemental composition from EDX and elemental analyses. This material is available free of charge via the Internet at http://pubs.acs.org.

REFERENCES AND NOTES

(1) Ahluwalia, R. K.; Wang, X. *J. Power Sources* **2008**, *177* (1), 167–176.
(2) Alberti, G.; Casciola, M.; Massinelli, L.; Bauer, B. *J. Membr. Sci.* **2001**, *185* (1), 73–81.
(3) Jannasch, P. *Curr. Opin. Colloid Interface Sci.* **2003**, *8*, 96–102.
(4) Li, Q.; He, R.; Jensen, J. O.; Bjerrum, N. J. *Chem. Mater.* **2003**, *15*, 4896–4915.
(5) Fernicola, A.; Navarra, M. A.; Panero, S. *J. Appl. Electrochem.* **2008**, *38* (7), 993–996.
(6) Martinelli, A.; Matic, A.; Jacobsson, P.; Boerjesson, L.; Fernicola, A.; Panero, S.; Scrosati, B.; Ohno, H. *J. Phys. Chem. B* **2007**, *111* (43), 12462–12467.
(7) Martinelli, A.; Matic, A.; Jacobsson, P.; Borjesson, L.; Navarra, M. A.; Panero, S.; Scrosati, B. *J. Electrochem. Soc.* **2007**, *154* (8), G183–G187.
(8) Schmidt, C.; Glueck, T.; Schmidt-Naake, G. *Chem. Eng. Technol.* **2008**, *31* (1), 13–22.
(9) Neves, L.; Dabek, W.; Coelhoso, I. M.; Crespo, J. G. *Desalination* **2006**, *199* (1−3), 525–526.
(10) Li, G.; Wang, L.; Ni, H.; Pittman, C. U. *J. Inorg. Organomet. Polym.* **2001**, *11* (3), 123–154.
(11) Phillips, S. H.; Haddad, T. S.; Tomczak, S. J. *Curr. Opin. Solid State Mater. Sci.* **2004**, *8* (1), 21–29.
(12) Fu, B. X.; Hsiao, B. S.; White, H.; Rafailovich, M.; Mather, P. T.; Jeon, H. G.; Phillips, S.; Lichtenhan, J.; Schwab, J. *Polym. Int.* **2000**, *49* (5), 437–440.
(13) Mariani, A.; Alzari, V.; Monticelli, O.; Pojman, J. A.; Caria, G. *J. Polym. Sci., Part A: Polym. Chem.* **2007**, *45* (19), 4514–4521.
(14) Xu, H.; Yang, B.; Wang, J.; Guang, S.; Li, C. *J. Polym. Sci., Part A: Polym. Chem.* **2007**, *45* (22), 5308–5317.
(15) Zhang, J.; Xu, R. W.; Yu, D. S. *J. Appl. Polym. Sci.* **2007**, *103* (2), 1004–1010.
(16) Chang, Y. W.; Wang, E.; Shin, G.; Han, J. E.; Mather, P. T. *Polym. Adv. Technol.* **2007**, *18* (7), 535–543.
(17) Hartmann-Thompson, C.; Merrington, A.; Carver, P. I.; Keeley, D. L.; Rousseau, J. L.; Hucul, D.; Bruza, K. J.; Thomas, L. S.; Keinath, S. E.; Nowak, R. M.; Katona, D. M.; Santurri, P. R. *J. Appl. Polym. Sci.* **2008**, *110* (2), 958–974.
(18) Choi, J. H.; Lee, K. M.; Wycisk, R.; Pintauro, P. N.; Mather, P. T. *ECS Trans.* **2008**, *16* (2), 1433–1442.
(19) Jiang, R.; Kunz, H. R.; Fenton, J. M. *J. Membr. Sci.* **2006**, *272*, 116–124.
(20) Pereira, F.; Valle, K.; Belleville, P.; Morin, A.; Lambert, S.; Sanchez, C. *Chem. Mater.* **2008**, *20* (5), 1710–1718.
(21) Tominaga, Y.; Hong, I.-C.; Asai, S.; Sumita, M. *J. Power Sources* **2007**, *171* (2), 530–534.
(22) Yen, C. Y.; Lee, C. H.; Lin, Y. F.; Lin, H. L.; Hsiao, Y. H.; Liao, S. H.; Chuang, C. Y.; Ma, C. C. M. *J. Power Sources* **2007**, *173* (1), 36–44.
(23) Ye, G.; Hayden, C. A.; Goward, G. R. *Macromolecules* **2007**, *40* (5), 1529–1537.
(24) Gomes, D.; Buder, I.; Nunes, S. P. *Desalination* **2006**, *199*, 274–276.
(25) Ladewig, B. P.; Knott, R. B.; Hill, A. J.; Riches, J. D.; White, J. W.; Martin, D. J.; Diniz da Costa, J. C.; Lu, G. Q. *Chem. Mater.* **2007**, *19* (9), 2372–2381.
(26) Lin, Y.-F.; Yen, C.-Y.; Ma, C.-C. M.; Liao, S.-H.; Lee, C.-H.; Hsiao, Y.-H.; Lin, H.-P. *J. Power Sources* **2007**, *171* (2), 388–395.
(27) Su, Y. Y.; Liu, Y. L.; Sun, Y. M.; Lai, J. Y.; Wang, D. M.; Gao, Y.; Liu, B.; Guiver, M. D. *J. Membr. Sci.* **2007**, *296* (1 + 2), 21–28.
(28) Su, Y. Y.; Wei, T. H.; Hsu, C. H.; Liu, Y. L.; Sun, Y. M.; Lai, J. Y. *Desalination* **2006**, *200* (1−3), 656–657.
(29) Carlier, E.; Revillon, A.; Guyot, A.; Baumgartner, P. *React. Polym.* **1993**, *21* (1−2), 15–25.
(30) Liu, L.; Song, L.; Zhang, S.; Guo, H.; Hu, Y.; Fan, W. *Mater. Lett.* **2006**, *60* (15), 1823–1827.
(31) Mauritz, K. A.; Moore, R. B. *Chem. Rev.* **2004**, *104* (10), 4535–4585.
(32) Gebel, G.; Diat, O. *Fuel Cells* **2005**, *5* (2), 261–276.
(33) Roche, E. J.; Pineri, M.; Duplessix, R. *J. Polym. Sci., Part A-2: Polym. Phys.* **1982**, *20* (1), 107–116.
(34) Roche, E. J.; Pineri, M.; Duplessix, R.; Levelut, A. M. *J. Polym. Sci., Part A-2: Polym. Phys.* **1981**, *19* (1), 1–11.
(35) Bennett, M. D.; Leo, D. J.; Wilkes, G. L.; Beyer, F. L.; Pechar, T. W. *Polymer* **2006**, *47* (19), 6782–6796.
(36) de Almeida, S. H.; Kawano, Y. *J. Therm. Anal. Calorim.* **1999**, *58*, 569–577.
(37) Thompson, E. L.; Capehart, T. W.; Fuller, T. J.; Jorne, J. *J. Electrochem. Soc.* **2006**, *153* (12), A2351–A2362.
(38) Corti, H. R.; Nores-Pondal, F.; Buera, M. P. *J. Power Sources* **2006**, *161* (2), 799–805.
(39) Nakajima, H.; Honma, I. *Solid State Ionics* **2002**, *148* (3−4), 607–610.
(40) Sacca, A.; Pedicini, R.; Carbone, A.; Gatto, I.; Passalacqua, E. *ECS Trans.* **2007**, *11* (1), 357–366.
(41) Paddison, S. J. *Annu. Rev. Mater. Res.* **2003**, *33* (1), 289–319.
(42) Park, M. J.; Downing, K. H.; Jackson, A.; Gomez, E. D.; Minor, A. M.; Cookson, D.; Weber, A. Z.; Balsara, N. P. *Nano Lett.* **2007**, *7* (11), 3547–3552.
(43) Hickner, M. A.; Pivovar, B. S. *Fuel Cells* **2005**, *5* (2), 213–229.
(44) Ye, H.; Huang, J.; Xu, J. J.; Kodiweera, N. K. A. C.; Jayakody, J. R. P.; Greenbaum, S. G. *J. Power Sources* **2008**, *178* (2), 651–660.

AM900020W